Title

Nrf2-related gene expression is impaired during a glucose challenge in type II diabetic rat hearts

Authors

Thorwald, Max A
Godoy-Lugo, Jose A
Rodriguez, Gema J
et al.

Publication Date

2019

DOI

10.1016/j.freeradbiomed.2018.10.405

Peer reviewed

Free Radical Biology and Medicine 130 (2019) 306–317

Contents lists available at ScienceDirect

Free Radical Biology and Medicine

journal homepage: www.elsevier.com/locate/freeradbiomed

Nrf2-related gene expression is impaired during a glucose challenge in type II diabetic rat hearts

Max A. Thorwald[a,b,*], Jose A. Godoy-Lugo[a], Gema J. Rodriguez[a], Marco Antonio Rodriguez[a], Mostofa Jamal[c], Hiroshi Kinoshita[c], Daisuke Nakano[d], Akira Nishiyama[d], Henry J. Forman[a,b], Rudy M. Ortiz[a]

[a] School of Natural Sciences, University of California, Merced, United States
[b] Leonard Davis School of Gerontology, University of Southern California, Los Angeles, CA, United States
[c] Department of Forensic Medicine, Kagawa University Medical School, Japan
[d] Department of Pharmacology, Kagawa University Medical School, Kagawa, Japan

ARTICLE INFO

Keywords:
Mitochondrial dysfunction
GSH
Nrf2
AT1
Hyperglycemia

ABSTRACT

Diabetic hearts are susceptible to damage from inappropriate activation of the renin angiotensin system (RAS) and hyperglycemic events both of which contribute to increased oxidant production. Prolonged elevation of oxidants impairs mitochondrial enzyme function, further contributing to metabolic derangement. Nuclear factor erythriod-2-related factor 2 (Nrf2) induces antioxidant genes including those for glutathione (GSH) synthesis following translocation to the nucleus. We hypothesized that an acute elevation in glucose impairs Nrf2-related gene expression in diabetic hearts, while AT1 antagonism would aid in Nrf2-mediated antioxidant production and energy replenishment. We used four groups (n = 6–8/group) of 25-week-old rats: 1) LETO (lean strain-control), 2) type II diabetic OLETF, 3) OLETF + angiotensin receptor blocker (ARB; 10 mg olmesartan/kg/d × 8 wks), and 4) ARBM (4 weeks on ARB, 4 weeks off) to study the effects of acutely elevated glucose on cardiac mitochondrial function and Nrf2 signaling in the diabetic heart. Animals were gavaged with a glucose bolus (2 g/kg) and groups were dissected at T0, T180, and T360 minutes. Nrf2 mRNA was 32% lower in OLETF rats compared to LETO and remained suppressed in response to glucose. LETO Nrf2 mRNA increased 25% at T360 in response to glucose while no changes were observed in diabetic hearts. GCLC and GCLM mRNA decreased in diabetic hearts 33% and 44% respectively and remained suppressed in response to glucose while ARB treatment increased GCLM transcripts 90% at T180. These data illustrate that during T2DM and in response to glucose, cardiac Nrf2's adaptive response to environmental stressors such as glucose is impaired in diabetic hearts and that ARB treatment may aid Nrf2's impaired dynamic response.

1. Introduction

Cardiovascular complications are the most common causes of mortality in type II diabetic (T2DM) patients implicating the diabetic heart as a risk factor [1]. The angiotensin II type 1 (AT1) receptor is inappropriately activated during T2DM contributing to the commonly associated hypertension and increased oxidant production [2]. Furthermore, it is known that hyperglycemia increases oxidant production through elevations in advanced glycation end products and through the polyol pathway [3,4]. Mitochondrial dysfunction occurs during insulin resistance and remains during T2DM reducing the efficiency of energy utilization and increasing oxidant production from aconitase oxidation or improper electron transfer from complex I to II and from II to I [5–7].

Nuclear factor (erythroid-derived 2)-like 2 (Nrf2) is retained in the cytosol through an interaction with Kelch-like ECH-associated protein 1 (Keap1). Oxidation of cysteines on Keap1 frees Nrf2, allowing it to translocate into the nucleus where it interacts with small maf proteins and binds to the electrophile response element (EpRE) to initiate transcription of antioxidant genes [8,9]. Several Antioxidants mitigate excessive oxidant production with the aid of NADPH which can be replenished through Nrf2-regulated pentose phosphate pathway enzymes [10]. During T2DM, Nrf2's translocation to the nucleus is impaired [11,12], which may contribute to impaired induction of antioxidants.

Glutathione (GSH), the most abundant non-enzymatic antioxidant in the body, protects the cell from oxidative injury and from xenobiotics. The GSH cycle can tag xenobiotics for degradation through

* Correspondence to: Department of Molecular & Cellular Biology, University of California Merced, 5200 N. Lake Rd., Merced, CA 95343, United States.
E-mail address: mthorwald@ucmerced.edu (M.A. Thorwald).

https://doi.org/10.1016/j.freeradbiomed.2018.10.405
Received 31 July 2018; Received in revised form 21 September 2018; Accepted 3 October 2018
Available online 11 October 2018
0891-5849/

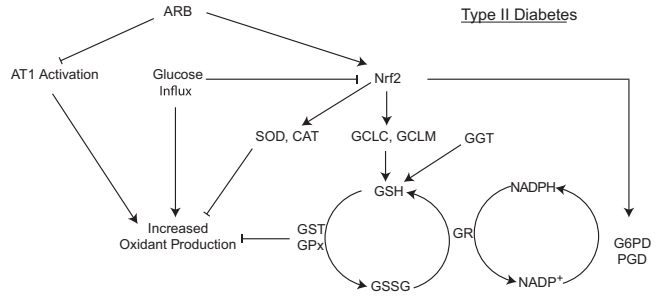

Scheme 1. Schematic representation of the proposed connection between the role of Nrf2 mediated antioxidants, oxidant generation from glucose, and inappropriate AT1 activation during Type II diabetes. Abbreviations: ARB = angiotensin receptor blocker, AT1 = angiotensin II type 1 receptor, CAT = catalase, G6PD = glucose 6-phosphate dehydrogenase, GCLC = glutathione cysteine ligase catalytic subunit, GCLM = glutathione cysteine ligase modifier subunit, GGT = gamma-glutamyl transferase, GPx = glutathione peroxidase, GR = glutathione reductase, GSH = reduced glutathione, GSSG = oxidized glutathione, GST = glutathione s-transferase, Nrf2 = Nuclear factor erythriod-2- related factor 2, PGD = phosphogluconate dehydrogenase, and SOD = superoxide dismutase.

glutathione s-transferase (GST), detoxify hydrogen peroxide through glutathione peroxidase (GPx), and reduce two oxidized GSH molecules (GSSG) through glutathione reductase (GR). GSH's production is regulated by glutamate cysteine ligase which has two subunits, glutamyl cysteine ligase catalytic (GCLC) and modifier (GCLM), which are primarily regulated by transcription factor Nrf2 (Scheme 1).

Hyperglycemia and hypertension are phenotypic of T2DM's pathology with both ailments impacting cardiovascular function [3,4,13]. Angiotensin receptor blockers (ARB) are prevalent for treatment of AT1 mediated hypertension which becomes inappropriately activated during insulin resistance and remains throughout T2DM pathology [13]. ARB treatment has been implicated in lowering oxidant production through lowering p47phox translocation [14]. While chronic ARB treatment during a glucose challenge in insulin resistant conditions increased Nrf2 nuclear binding and improved cardiac mitochondrial function [15,16], the possible benefits of chronic ARB treatment on Nrf2 signaling and mitochondrial function during a glucose challenge in T2DM hearts has not been explored. Additionally, the significance of compliance and the "cell memory" or "legacy effect" with respect to AT1 signaling during T2DM has not been examined [17,18]. We hypothesized that an acute elevation in glucose impairs Nrf2-related gene expression in diabetic hearts, while AT1 antagonism would aid in Nrf2-mediated antioxidant production and energy replenishment. The goals of this study were: (1) to elucidate the dynamic Nrf2 response in normal and diabetic hearts in response to glucose, (2) to assess the effects of chronic blockade of AT1 on acutely elevated glucose-induced changes in Nrf2 regulation and mediation, and (3) to evaluate the potential consequences of non-compliance in ARB treatment and potential legacy effects during aforementioned conditions.

2. Methods

All experimental procedures were reviewed and approved by the institutional animal care and use committees of Kagawa Medical University (Kagawa, Japan), and the University of California, Merced.

2.1. Animals

Male, age matched, 17-week-old, lean strain-control Long Evans Tokushima Otsuka (LETO; 428 ± 8 g) and obese Otsuka Long Evans Tokushima Fatty (OLETF; 536 ± 6 g) rats (Japan SLC Inc., Hamamatsu, Japan) were chosen because OLETF rats have been previously shown to develop insulin resistance and hyperglycemia by 17 weeks of age and frank, T2DM by 24 weeks of age [2]. LETO and OLETF rats were assigned to the following groups (n = 6–8 animals/group/time point): 1) untreated LETO, 2) untreated OLETF, and 3) OLETF + angiotensin receptor blocker (ARB; 10 mg olmesartan/kg/d × 8 wk), and 4) OLETF ± ARB (10 mg olmesartan/kg/d × 4 wks then removed until dissection). The ARB removal group allowed us to assess the impacts of compliance and potential legacy effects [17,18] with respect to AT1 signaling, which has not be studied under T2DM conditions. ARB (Daiichi-Sankyo, Tokyo, Japan) was administered by oral gavage suspended in carboxymethyl cellulose (CMC) to conscious rats [15]. Untreated LETO and OLETF rats were gavaged with CMC only. All animals were maintained in groups of two to three animals per cage in a specific pathogen-free facility under controlled temperature (23 °C) and humidity (55%) with a 12-h light, 12-h dark cycle. All animals were given free access to water and standard laboratory rat chow (MF; Oriental Yeast Corp., Tokyo, Japan).

2.2. Body mass (BM) and food consumption

BM and food consumption were measured every other day starting at week 17 through the end of the study to help confirm the diet-induced obesity phenotype typical of the model. BM was also used to determine the appropriate dosage of ARB for treated animals (10 mg/kg/d) [15,16,19,20]. Food intake was estimated as the average per cage.

2.3. Blood pressure

Systolic blood pressure (SBP) was measured weekly, starting at week 17 until the end of the study (25 weeks) in conscious rats by tail-cuff plethysmography (BP-98A; Softron Co., Tokyo, Japan) to confirm the inappropriate elevation in RAS, which is associated with this model [15,16,19–21].

2.4. Glucose tolerance tests

One week prior to dissections (24 weeks), rats were fasted overnight for 12 h and gavaged with glucose (2 g/kg) to assess the degree of glucose intolerance. Blood was collected for plasma glucose and insulin as previously described [20]. We subsequently calculated area under the curves for glucose and insulin which helped confirm the diabetic status of the animals.

3. Dissections

Animals were dissected at 25 weeks of age because OLETF rats have been shown to be diabetic by 24 weeks [2,22]. Food was removed from the cages at 12 h before dissection. Cages were staggered to ensure that all rats were fasted for 12 h ± 15 min. Dissections were performed at baseline (T0), and 3 (T180) and 6 h post-glucose (T360). Oral glucose challenges were also staggered to ensure punctuality for the respective dissection times. Animals were decapitated and trunk blood was collected into chilled vials containing 50 mM EDTA and protease inhibitor cocktail (Sigma, St. Louis, MO) and kept on ice until tubes were centrifuged. Hearts were perfused with saline and rapidly removed, weighed, and snap frozen in liquid nitrogen. The remaining ventricle and plasma were kept at −80 °C until analyzed.

3.1. GSH measurements

200 mg of heart tissue from the apex of the heart was quickly homogenized in 0.6% sulfosalicylic acid at the time of dissection for deproteination [23]. Samples were then extracted and GSH was measured by electrochemical detection using a Eicom HPLC ECD-300 (Eicom, Kyoto, Japan) as previously described [24].

3.2. Western blot analyses

A 15–25 mg piece of frozen heart was homogenized in 150 uL of sucrose buffer for extraction of mitochondrial, nuclear, and cytosolic fractions [25]. Total protein content of the fractions was measured by the Bradford assay (Bio-Rad Laboratories, Hercules, CA). Five to thirty micrograms of total protein were resolved in 4–15% Tris-HCl SDS gradient gels. Proteins were electroblotted using the Bio-Rad wet transfer onto 0.45-μm polyvinyl difluoride membranes. Membranes were blocked with LI-COR Odyssey blocking buffer and incubated for 16 h with primary antibodies (diluted 1:100–1:4000) against GCLC, GCLM (provided by Dr. Forman), acetylated-Nrf2 (Elabscience, Houston, Tx), and Keap1, Nrf2, GSK3β, NT, Parkin (Santa Cruz Biotechnology, Santa Cruz, CA). Membranes were washed, incubated with IRDye 800CW and/or 700CW donkey anti-goat, donkey anti-mouse, or donkey anti-rabbit (LI-COR Biosciences, Lincoln, NE), and rewashed. Blots were visualized using an Odyssey system (LI-COR Biosciences) and quantified using ImageJ. Nuclear and cytosolic extractions were performed and tested for purity against H3 and GAPDH in both fractions [25]. Mitochondrial extractions were also tested for purity with VDAC1 and GAPDH. In addition to consistently loading the same amount of total protein per well, the densitometry values were further normalized by correcting with the densitometry values by Ponceau S staining [26].

3.3. Real-time quantitative PCR analyses

Total RNA was obtained using TRIzol reagent (Invitrogen, Carlsbad, CA). Genomic DNA was degraded on the samples using DNase I enzyme (Roche, Indianapolis, IN). Complementary DNA was reverse transcribed from gDNA-free RNA using the High-Capacity cDNA Reverse Transcription Kit (Applied Biosystems, Foster City, CA) using oligio-dT. Real-time PCR reactions were performed in duplicates, using an equivalent to 100 ng of RNA per reaction, using specific primers for Keap1, GSK3β, Nrf2, Bach1, c-Myc, G6PD, PGD, GCLM, GCLC, and normalized with B2M expression. Primer sequences used for qPCR analyses are shown in Table 1.

3.4. Biochemical analyses

Activities of plasma GGT (BIOO Scientific, Austin, TX), nuclear Nrf2 (Active Motif, Carlsbad, CA), and citric acid cycle and antioxidant enzymes (aconitase, CAT, GPx, SOD, GR, and GST) (Cayman Chemical, Ann Arbor, MI) were measured using commercially available kits as previously described [15]. Complex I, Complex II, NADPH ratios, NADH ratios (Abcam, Cambridge, MA), and insulin (Morinaga, Yokohama-Shi, Japan) assays were measured by commercial ELISAs. NADH and NADPH were measured immediately after dissection to avoid sample degradation. All samples were analyzed in duplicate and run in a single assay with intra-assay and percent coefficients of variability of less than 10% for all assays.

Table 1
Primer sequences used for real time PCR.

Primer name	Nucleotide sequence (5′-3′)
Keap1-F	ATGTGATGAACGGGGCAGTC
Keap1-R	AGAACTCCTCCTCCCCGAAG
Gsk3b-F	CTGGCCACCATCCTTATCCC
Gsk3b-R	GAAGCGGCGTTATTGGTCTG
Nrf2-F	ATTTGTAGATGACCATGAGTCGC
Nrf2-R	TGTCCTGCTGTATGCTGCTT
Bach1-F	CACAAAGTGCAAAGACCCCG
Bach1-R	ATCGCCTGACTGCTCGTATG
c-Myc-F	CAGCTCGCCCAAATCCTGTA
c-Myc-R	GCCTCTTGATGGGGATGACC
G6pd-F	GAGGACCAGATCTACCGC
G6pd-R	CAAAATAGCCCCCACGACC
Pgd-F	GCTGACATTGCACTGATTGG
Pgd-R	TCACGAGCAGTATGACCCG
Gclm-F	GTTCATTGTAGGATCG
Gclm-R	GGTGCCTATAGCAACAATCT
Gclc-F	CTGGACTCATCCCCATTC
Gclc-R	GTAGTCAGGATGGTTTGC
B2m-F	ATGGGAAGCCCAACTTCCTC
B2m-R	ATACATCGGTCTCGGTGGGT

3.5. Statistics

Means (± SEM) were compared by ANOVA. Means were considered significantly different at $P < 0.05$ using Tukey's HSD. Statistical analyses were performed with SYSTAT 13 software (SYSTAT, San Jose, CA).

4. Results

4.1. AT1 activation increases ventricular hypertrophy

Relative food consumption was 57% higher in OLETF rats compared to LETO (Table 2). Treatment had no discernable effect on relative food consumption compared to OLETF. Body mass was 35% higher in OLETF rats compared to LETO with no difference amongst treatment groups (Table 2). Absolute ventricular mass increased 15% in OLETF rats compared to LETO (Table 2). ARB treatment lowered absolute ventricular mass by 10% while ARBM treatment returned ventricular mass to OLETF levels. Relative ventricular mass was not different between LETO and OLETF, but ARB treatment decreased relative ventricular mass 8% and removal of ARB treatment return levels to OLETF (Table 2).

4.2. ARB effectively blocked the AT1 receptor

Mean SBP increased 42% in OLETF compared to LETO, and while ARB treatment completely ameliorated the elevated arterial pressure, removal of ARB completely restored the hypertension (Fig. 1A). Plasma angiotensin II was measured to assess the ARB's efficacy. At T0, plasma angiotensin II was 4-fold higher in ARB compared to OLETF. ARBM treatment restored plasma angiotensin II values to OLETF levels (Fig. 1B).

4.3. ARB treatment improves glucose tolerance and insulin response

Glucose and Insulin levels were measured a week prior to dissection to ensure that the rats were diabetic prior to dissection. Plasma glucose and insulin were measured during the oral glucose tolerance test to assess the degree of glucose intolerance and insulin resistance in type II diabetic rats (Fig. 2A, C). Plasma glucose area under the curve ($AUC_{glucose}$) was 195% higher in OLETF rats compared to LETO. ARB treatment lowered $AUC_{glucose}$ 19% and ARB removal lowered $AUC_{glucose}$ 21% (Fig. 2B). Insulin AUC ($AUC_{insulin}$) more than doubled in OLETF rats compared to LETO, and ARB treatment lowered $AUC_{insulin}$ 30%, while removal of ARB was not different from OLETF or ARB indicative of an intermediary phenotype (but more similar to ARB) (Fig. 2D).

4.4. Diabetes suppresses Nrf2 signaling, but is not profoundly altered with ARB treatment

Nrf2 translocation, acetylation, and several of its regulators were measured to gain a better understanding of the impact of an acute glucose challenge on Nrf2 signaling. At T0, Nrf2 mRNA was 32% lower in OLETF rats compared to LETO (Fig. 3A). Nrf2 mRNA was 27% lower in OLETF compared to LETO rats at T180, while ARB treated animals were 51% lower compared to OLETF. ARBM treatment returned Nrf2 mRNA transcripts to OLETF levels at T180. At T360, Nrf2 transcripts

Table 2
Mean ± SEM for food consumption, BM, heart mass and relative heart mass in Long Evans Tokushima Otsuka (LETO; n = 6), Otsuka Long Evans Tokushima Fatty (OLETF; n = 8), OLETF + angiotensin receptor type 1 blocker 8 weeks (ARB; n = 8) rats, and OLETF + angiotensin receptor type 1 blocker 4 weeks, then removed (ARBM; n = 8) rats. Relative heart mass SEM values are less than 0.01.

	LETO	OLETF	ARB	ARBM
Food consumption (g)	20.2 ± 0.6	31.8 ± 1.0*	30.8 ± 0.7	32.5 ± 0.4
Body mass (g)	481 ± 7	650 ± 7*	632 ± 5	631 ± 6
Ventricular mass (g)	1.34 ± 0.06	1.54 ± 0.02*	1.39 ± 0.02†	1.53 ± 0.02¥
Relative ventricular mass (g/kg)	0.27 ± 0.01	0.25 ± 0.01*	0.23 ± 0.01†	0.25 ± 0.01¥

* Significant difference from LETO ($P < 0.05$).
† Significant difference from OLETF ($P < 0.05$).
¥ Significant difference between OLETF and ARBM ($P < 0.05$).

were 41% lower in OLETF compared to LETO rats. At T360, glucose increased Nrf2 transcripts 25% from T0 and T180 in LETO rats. In ARB treated animals, glucose lowered Nrf2 transcripts 56% at T180 compared to T0 (Fig. 3A). At T0, cytosolic Nrf2 content was 50% lower in OLETF rats compared to LETO (Fig. 3B). At T0, ARB and ARBM treatments increased cytosolic Nrf2 content 213% and 151%, respectively (Fig. 3B). At T180, glucose increased cytosolic Nrf2 protein 173% in OLETF rats (Fig. 3B). No statistical differences were detected in nuclear Nrf2 protein content among the groups (Fig. 3C). At T0, Nrf2 acetylation increased 30% and 42% in ARB and ARBM treated animals, respectively, compared to OLETF (Fig. 3D). Glucose increased LETO Nrf2 acetylation 48% and 34% at T180 and T360, respectively, compared to T0. At T0, GSK3β mRNA transcripts were nearly 30-fold higher in ARBM treated animals compared to OLETF and ARB (Fig. 3E). At T180, GSK3β transcripts increased over 40-fold in ARB animals compared to OLETF, and 75-fold and 83% higher in ARBM compared to OLETF and ARB animals, respectively. At T360, GSK3β transcripts were approximately 36- and 29-fold higher in ARB and ARBM treatment groups, respectively, compared to OLETF. In ARB treated animals, glucose increased GSK3β transcripts approximately 18- and 29-fold at T180 and T360, respectively (Fig. 3E). At T0, GSK3β protein was 84% higher in OLETF rats compared to LETO (Fig. 3F). In LETO, GSK3β was 33% higher at T180 compared to T0, and decreased 16% at T360 (Fig. 3F). At T0, Keap1 mRNA transcripts were 55% and 98% lower in ARB and ARBM treated animals, respectively, compared to OLETF (Fig. 3G). At T0, Keap1 transcripts were 96% lower in ARBM treatment compared ARB (Fig. 3G). At T180, Keap1 mRNA decreased 69% in OLETF compared LETO, while ARB treatment increased transcripts by 73%. At T180, Keap1 mRNA was 97% and 99% lower in ARBM treated animals compared to OLETF and ARB treated animals, respectively. At T360, Keap1 transcripts were 94% lower in OLETF compared to LETO. In LETO, Keap1 transcripts were 105% higher at T360 compared to T0. In OLETF, glucose suppressed Keap1 transcripts 29% at T180 and 82% at T360 compared to T0. At T180, Keap1 transcripts in ARB treated animals increased nearly 5-fold compared to T0, but decreased 91% at T360 (Fig. 3G). At T0, Keap1 protein was 22% lower in ARB treated animals compared to OLETF, while ARBM treatment increased Keap1 protein 42% compared to ARB (Fig. 3H). At T0, Keap1 protein in ARBM treatment was 41% greater compared to ARB. In ARB treatment, Keap1 protein increased 45% at T180, and deceased 31% and 52% at T360 compared T0 and T180, respectively (Fig. 3H). At T180, Bach1 mRNA transcripts decreased 64% in OLETF rats compared to LETO (Fig. 3I). In ARB treated animals, glucose increased Bach1 transcripts at T360 by 64% and 194% compared T0 and T180, respectively (Fig. 3I). At T0, c-Myc mRNA transcripts was 50% lower in OLETF rats compared to LETO (Fig. 3J). At T0, c-Myc transcripts were 83% and 84% lower in ARBM treatment compared to OLETF and ARB treatment, respectively. At T180 and T360, transcripts were 48% and 57% lower, respectively, in OLETF compared to LETO (Fig. 3J). In ARB treated animals, glucose increased c-Myc transcripts over 7- and 5-fold at T180 and T360, respectively, compared to T0 (Fig. 3J).

4.5. Oxidant detoxification increased in mitochondrial antioxidant activities while cytosolic remains unchanged

Antioxidant activities were measured in both the cytosol and the mitochondria to elucidate the impact of glucose on antioxidants during T2DM. to At T0, Mitochondrial SOD activity increased 38% in ARB treated animals compared to OLETF (Fig. 4A). Mitochondrial SOD levels were 20% lower in ARBM treated animals compared to ARB treatment at T0 (Fig. 4A). Mitochondrial SOD activity increased 34% in OLETF rats compared to LETO at T180 (Fig. 4A). At T180 ARBM treated animals had 33% lower mitochondrial SOD levels than OLETF and ARB treated rats respectively. Glucose increased LETO mitochondrial SOD activity at T180 20% compared to T0. Glucose increased OLETF mitochondrial SOD levels 42% at T180 and decreased activity at T360 by

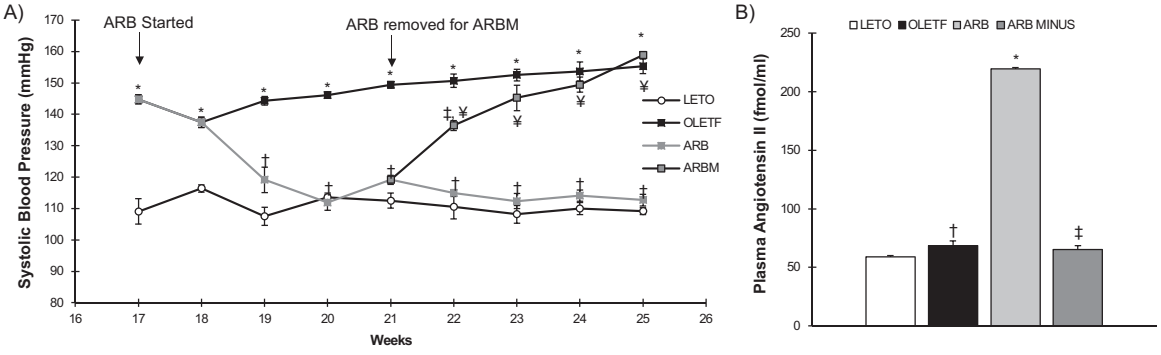

Fig. 1. Systolic blood pressure and angiotensin levels. Mean ± SEM values of A) Systolic blood pressure starting from 17 weeks until 25 weeks of age, and B) plasma angiotensin II levels post glucose challenge in Long Evans Tokushima Otsuka (LETO; n = 6), Otsuka Long Evans Tokushima Fatty (OLETF; n = 8), OLETF + angiotensin receptor type 1 blocker 8 weeks (ARB; n = 8) rats, and OLETF + angiotensin receptor type 1 blocker 4 weeks, then removed (ARBM; n = 8) rats. *Significant difference from LETO ($P < 0.05$). † Significant difference from OLETF ($P < 0.05$). ‡ Significant difference from ARB ($P < 0.05$). ¥ Significant difference between OLETF and ARBM ($P < 0.05$).

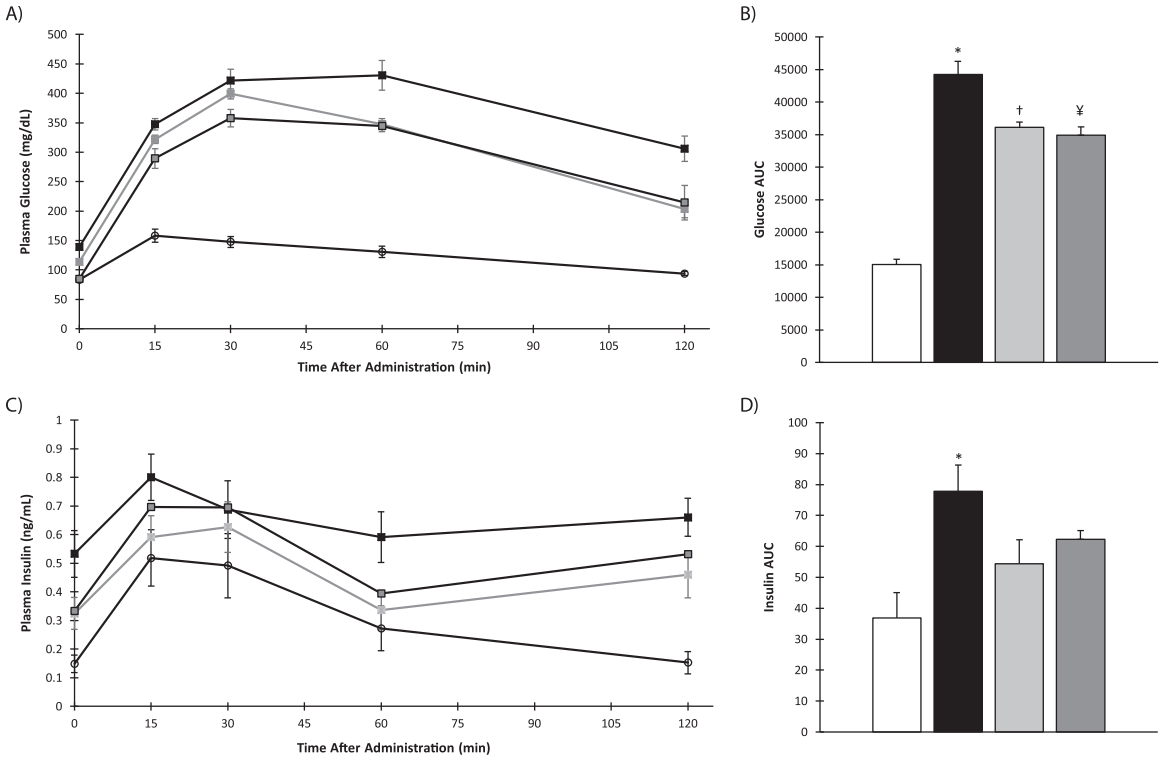

Fig. 2. Glucose and Insulin tolerance. Mean ± SEM values of A) plasma glucose levels, B) glucose area under the curve values, C) plasma insulin levels, and D) insulin under the curve values post glucose challenge in Long Evans Tokushima Otsuka (LETO; n = 6), Otsuka Long Evans Tokushima Fatty (OLETF; n = 8), OLETF + angiotensin receptor type 1 blocker 8 weeks (ARB; n = 8) rats, and OLETF + angiotensin receptor type 1 blocker 4 weeks, then removed (ARBM; n = 8) rats. *Significant difference from LETO ($P < 0.05$). † Significant difference from OLETF ($P < 0.05$). ¥ Significant difference between OLETF and ARBM ($P < 0.05$).

19%. Glucose decreased mitochondrial SOD activity 25% at T360 compared to T180 in ARB treated animals (Fig. 4A). Cytosolic SOD was 25% higher in ARBM treated animals compared to OLETF at T0 (Fig. 4B). Cytosolic SOD activity was 17% lower in ARB treated animals compared to OLETF rats at T180 while ARBM treated rats were 24% higher (Fig. 4B). Glucose suppressed cytosolic SOD activity 18% in ARBM treated rats at T360 compared to T0 (Fig. 4B). Mitochondrial CAT activity was 85% higher in OLETF rats compared to LETO at T180, while ARB treated animals were the same as LETO animals (Fig. 4C). Glucose increased mitochondrial CAT activity 85% in OLETF rats at T180 compared to T0. Glucose suppressed mitochondrial CAT levels 49% and 40% respectively in OLETF and ARBM treated animals at T360 compared to T180 (Fig. 4C). No significant changes were observed with cytosolic CAT activity over the 6-h time frame (Fig. 4D).

4.6. AT1 blockade promotes GSH synthesis during the diabetic condition and is impaired with ARB removal

GSH, and several components of the GSH cycle were measured to examine the dynamic changes that occur in response to an acute glucose challenge. At T0, total GSH levels increased 26% in ARB treated rats compared to OLETF (Fig. 5A). In LETO, glucose suppressed GSH levels 20% and 26% at T180 and T360, respectively, but increased GSH levels 27% and 80% at T180 and T360, respectively, in OLETF. Thus, GSH levels were 68% higher at T180 and 157% higher at T360 in OLETF compared to LETO. At T360, GSH levels were 33% and 31% lower with ARBM treatment compared to OLETF and ARB treated rats, respectively (Fig. 5A). In ARB treated animals, glucose increased GSH content 39% and 38% at T360 compared to T0 and T180, respectively (Fig. 5A). At T0, plasma GGT activity was 38% lower in OLETF rats compared to LETO, and ARB treatment or removal had no effect (Fig. 5B). In LETO, glucose increased plasma GGT activity 41% and 35% at T180 and T360, respectively, relative to T0, and 57% and 77% at T180 and T360, respectively, relative to T0 in OLETF. In ARB treated rats, glucose increased plasma GGT activity 84% and 85% at T180 and T360, respectively, relative to T0, and increased activity 98% at T360 only relative to T0 in ARBM treatment (Fig. 5B). At T180, plasma GGT activity was 32% lower in OLETF than LETO (Fig. 5B). At T0, GCLC mRNA transcripts were decreased 39% in OLETF compared to LETO, while ARBM treatment increased transcripts by 49% (Fig. 5C). In OLETF, GCLC transcripts remained 35% lower than LETO at T180. In LETO, glucose increased GCLC transcripts by 28% and 39% and 35% and 56% in OLETF at T180 and T360, respectively (Fig. 5C). At T0, GCLC protein levels were 33% lower in OLETF rats compared to LETO (Fig. 5D). At T0, GCLM mRNA transcripts were 44% lower in OLETF animals compared to LETO (Fig. 5E). At T0, ARB treatment increased GCLM transcripts 35% compared to OLETF. At T0, GCLM transcripts were 89% and 92% lower in ARBM treatment compared to OLETF and ARB treated rats, respectively (Fig. 5E). At T180, glucose increased GCLM transcripts by 90% in ARB treatment compared to OLETF, while GCLM transcripts were 88% and 94% lower in ARBM treatment compared to OLETF and ARB treated rats, respectively (Fig. 5E). At T360, transcripts were 60% lower in OLETF than LETO, and 70% lower in ARB treated rats than OLETF. In ARBM treatment, GCLM transcripts were 90% and 67% lower than OLETF and ARB treated animals, respectively. At T180, glucose increased GCLM transcripts by 108% in ARB treatment, and decreased 91% at T360 (Fig. 5E). In LETO, glucose increased GCLM transcripts 24% at T360. In ARB treatment, glucose increased transcripts 108% at T180 and decreased them 91% at T360 (Fig. 5E). In ARBM treatment, glucose increased GCLM transcripts by 67% at T180 and decreased them 51% at T360 (Fig. 5E). At T0 GCLM protein levels were 39% lower in OLETF rats compared to LETO, while GCLM levels were restored in ARB treated rats (Fig. 5F). In LETO, glucose suppressed GCLM protein levels 24% at T360, and 24% and 35% at T180 and T360, respectively, in ARB treated animals (Fig. 5F). Mitochondrial GPx activity was lower 44% and 49% at T180 in ARBM

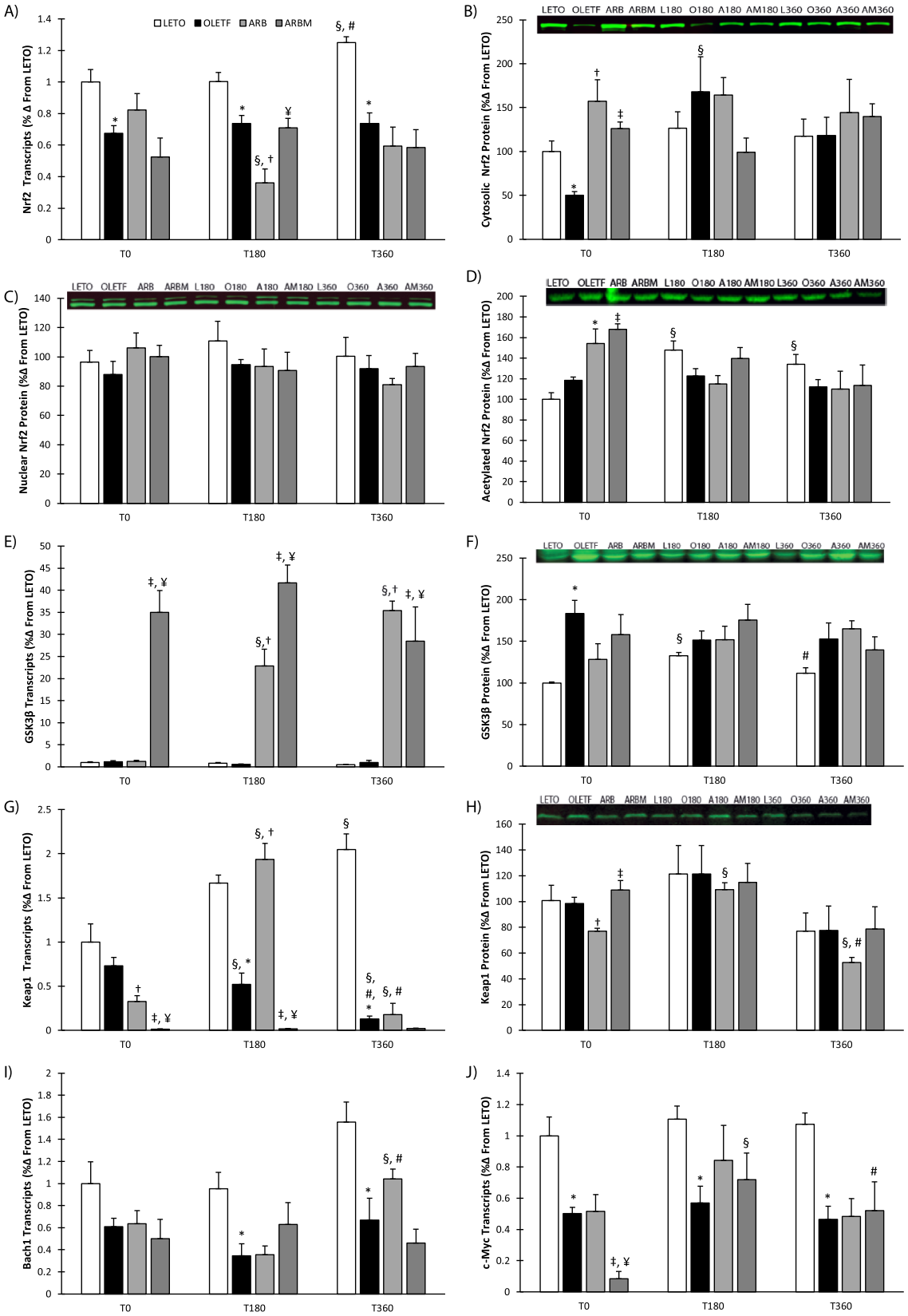

Fig. 3. Nrf2 signaling. Mean ± SEM values of A) Nrf2 transcripts, B) cytosolic Nrf2 protein, C) nuclear Nrf2 protein, D) acetylated-Nrf2 protein, E) GSK3β transcripts, F) GSK3β protein, G) Keap1 transcripts, H) Keap1 protein, I) Bach1 transcripts, and J) c-Myc mRNA values post glucose challenge in Long Evans Tokushima Otsuka (LETO; n = 6), Otsuka Long Evans Tokushima Fatty (OLETF; n = 8), OLETF + angiotensin receptor type 1 blocker 8 weeks (ARB; n = 8) rats, and OLETF + angiotensin receptor type 1 blocker 4 weeks, then removed (ARBM; n = 8) rats. §Significant difference from respective T0 ($P < 0.05$). #Significant difference from respective T180 ($P < 0.05$). *Significant difference from LETO ($P < 0.05$). † Significant difference from OLETF ($P < 0.05$). ‡ Significant difference from ARB ($P < 0.05$). ¥ Significant difference between OLETF and ARBM ($P < 0.05$).

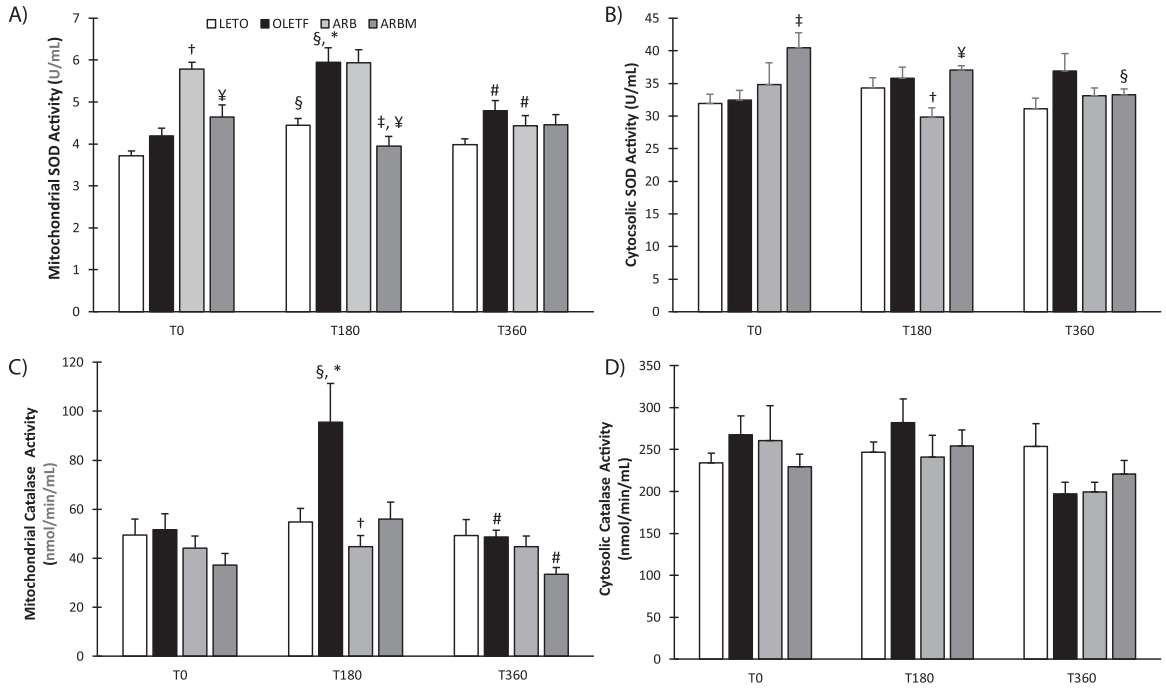

Fig. 4. Superoxide dismutase and catalase activities in the cytosol and mitochondria. Mean ± SEM values of A) mitochondrial SOD activity, B) cytosolic SOD activity, C) mitochondrial CAT activity, and D) cytosolic CAT activity values post glucose challenge in Long Evans Tokushima Otsuka (LETO; n = 6), Otsuka Long Evans Tokushima Fatty (OLETF; n = 8), OLETF + angiotensin receptor type 1 blocker 8 weeks (ARB; n = 8) rats, and OLETF + angiotensin receptor type 1 blocker 4 weeks, then removed (ARBM; n = 8) rats. §Significant difference from respective T0 ($P < 0.05$). #Significant difference from respective T180 ($P < 0.05$). *Significant difference from LETO ($P < 0.05$). † Significant difference from OLETF ($P < 0.05$). ‡ Significant difference from ARB ($P < 0.05$). ¥ Significant difference between OLETF and ARBM ($P < 0.05$).

treated animals compared to OLETF and ARB treated animals (Fig. 5G). At T360 ARBM animals had 28% lower mitochondrial GPx activity compared to OLETF treatment. Glucose suppressed mitochondrial GPx activity in ARBM treated rats at T180 28% compared to T0 (Fig. 5G). No significant changes were observed in cytosolic GPx activity in response to glucose (Fig. 5H). Mitochondrial GR levels increased in OLETF rats at T180 153% compared to LETO (Fig. 5I). Mitochondrial GR levels increased 72% in ARB treated animals compared to OLETF at T180, while ARBM treated animals had 70% less GR activity than ARB treatment. Glucose increased LETO mitochondrial GR 90% by T360 compared to T180. Glucose increased mitochondrial GR activity 59% at T180 which then decreased it 54% and 71% by T360 compared to T0 and T180 in ARB treated animals (Fig. 5I). Cytosolic GR activity in OLETF rats was 21%, 20%, and 28% lower than LETO rats at T0, T180, and T360 respectively (Fig. 5J). Glucose increased LETO cytosolic GR activity 16% at T360 compared to T0 and T180 respectively (Fig. 5J). Mitochondrial GST was 41% lower in ARBM treated animals compared to ARB treatment at T0 (Fig. 5K). Glucose suppressed mitochondrial GST activity in ARB treated animals 44% at T180. LETO mitochondrial GST activities increased 12% at T360 compared to T180 (Fig. 5K). No significant changes were observed with cytosolic GST activity over the 6-h time frame (Fig. 5L).

4.7. NADPH replenishment is downregulated during diabetes but is improved with AT1 antagonism

Enzymes in the oxidative phase of the pentose phosphate pathway were measured because they're under Nrf2's regulation and aid in producing NADPH. At T0, G6PD mRNA transcripts in OLETF were 48% lower compared to LETO, and glucose reduced them 56% at T180 compared to LETO (Fig. 6A). At T0, PGD mRNA transcripts were 41% lower in OLETF rats compared to LETO (Fig. 6B). In LETO, glucose increased PGD transcripts 53% and 70% at T360 compared T0 and T180, respectively (Fig. 6B). At T360, PGD mRNA was 68% lower in OLETF rats compared to LETO. At T180, PGD mRNA was 137% higher in ARBM treated animals compared to OLETF (Fig. 6B). At T0, ARB treatment lowered $NADP^+$/NADPH ratios 37% compared to OLETF, but no strain effect was detected (Fig. 6C). At T360, glucose increased $NADP^+$/NADPH ratios 61% in OLETF compared to LETO and decreased the ratio 18% in ARB treatment and were decreased an additional 34% in ARBM treatment (Fig. 6C). At T360, glucose increased the ratio of $NADP^+$/NADPH 42% and 86% in OLETF and ARB treated rats, respectively (Fig. 6C).

4.8. AT1 antagonism does not provide any benefit to mitochondrial enzyme activities

Several mitochondrial enzymes were measured to examine the impact of a glucose challenge on diabetic mitochondrial function. Aconitase activity was increased 186% in OLETF rats compared to LETO at T360 (Fig. 7A). ARB treated animals had 23% lower aconitase activity at T360 compared to OLETF (Fig. 7A). Complex I activity was 32% lower in OLETF rats compared to LETO at T0 (Fig. 7B). OLETF complex I activity remained lower by 17% and 29% compared to LETO at T180 and T360 respectively (Fig. 7B). Glucose suppressed OLETF complex I activity by 14% at T360 compared to T180 (Fig. 7B). Glucose complex I activity by 25% at T360compared to T180 in ARB treated rats (Fig. 7B). Glucose increased OLETF complex II activity 47% at T180 and suppressed activity 35% by T360 (Fig. 7C). At T0, ARB treatment increased NAD^+/NADH ratios by 33% compared to OLETF, but no strain effect was detected (Fig. 7D). In LETO, glucose lowered NAD^+/NADH ratio 31% at T180, but increased it 97% at T360. At T180, glucose suppressed NAD^+/NADH ratio 59% in ARB treated rats compared to OLETF, and ARB removal returned the ratio to OLETF levels. At T360, the ratio was 53% and 37% higher in ARBM treatment than OLETF and ARB treated rats, respectively (Fig. 7D). At T180, glucose lowered NAD^+/NADH ratio 77% in ARB treated rats but increased them nearly 3-fold at T360. At T180, glucose lowered NAD^+/NADH ratio 33% in

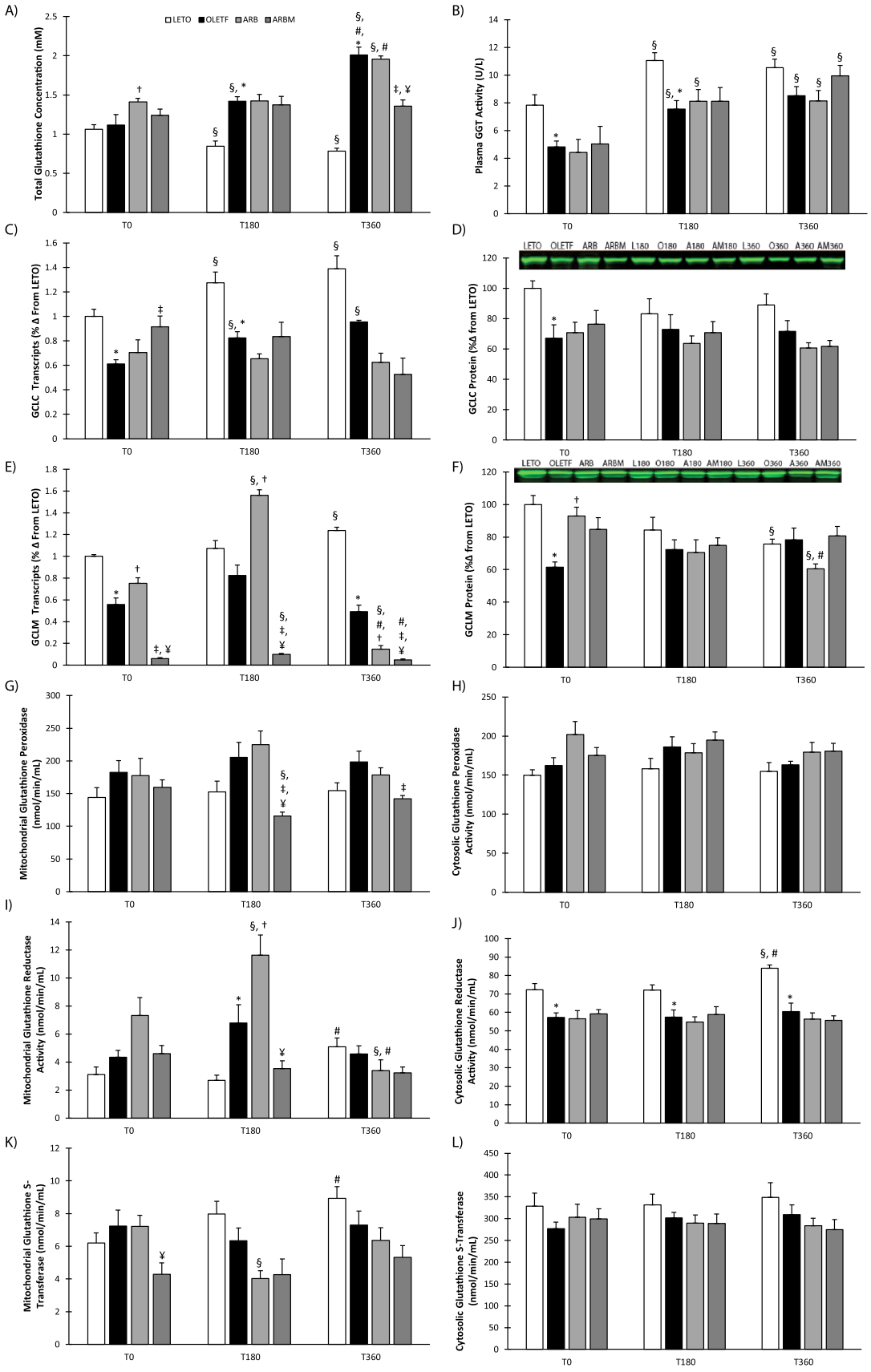

(caption on next page)

Fig. 5. GSH Cycle. Mean ± SEM values of A) total GSH levels, B) plasma GGT activity, C) GCLC transcripts, D) GCLC protein, E) GCLM transcripts, F) GCLM transcripts, G) mitochondrial GPx activity, H) cytosolic GPx activity, I) mitochondrial GR activity, J) cytosolic GR activity, K) mitochondrial GST activity, and L) cytosolic GST activity values post glucose challenge in Long Evans Tokushima Otsuka (LETO; n = 6), Otsuka Long Evans Tokushima Fatty (OLETF; n = 8), OLETF + angiotensin receptor type 1 blocker 8 weeks (ARB; n = 8) rats, and OLETF + angiotensin receptor type 1 blocker 4 weeks, then removed (ARBM; n = 8) rats. §Significant difference from respective T0 ($P < 0.05$). #Significant difference from respective T180 ($P < 0.05$). *Significant difference from LETO ($P < 0.05$). † Significant difference from OLETF ($P < 0.05$). ‡ Significant difference from ARB ($P < 0.05$). ¥ Significant difference between OLETF and ARBM ($P < 0.05$).

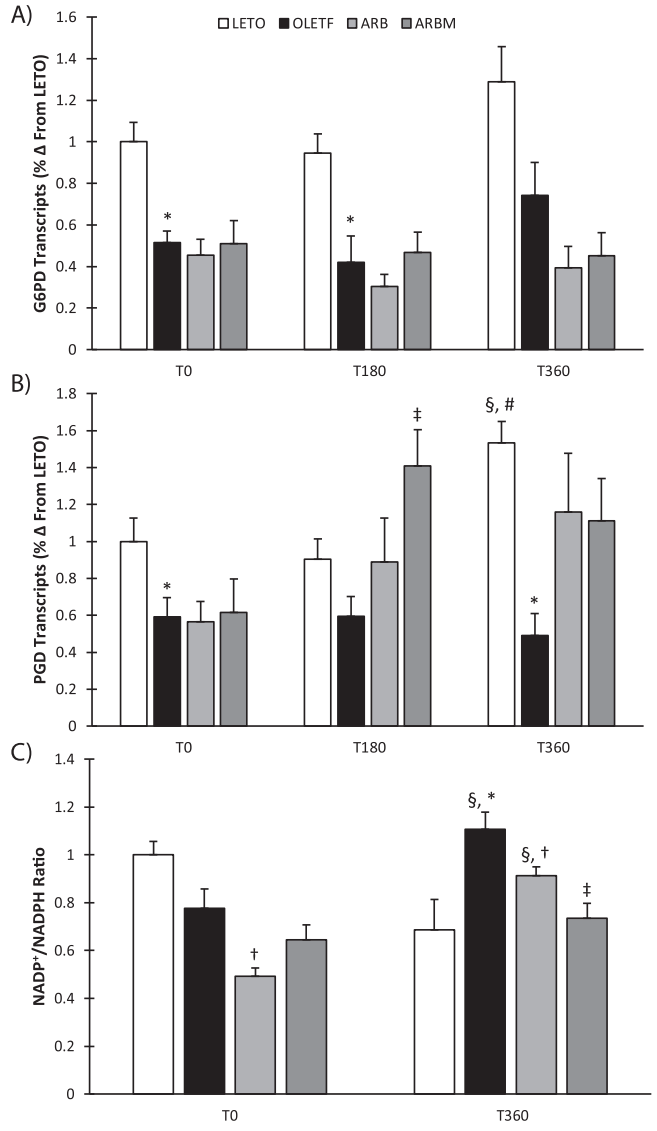

Fig. 6. Pentose phosphate pathway and NADPH status. Mean ± SEM values of A) G6PD transcripts, B) PGD transcripts, and C) $NADP^+$/NADPH ratio values post glucose challenge in Long Evans Tokushima Otsuka (LETO; n = 6), Otsuka Long Evans Tokushima Fatty (OLETF; n = 8), OLETF + angiotensin receptor type 1 blocker 8 weeks (ARB; n = 8) rats, and OLETF + angiotensin receptor type 1 blocker 4 weeks, then removed (ARBM; n = 8) rats. §Significant difference from respective T0 ($P < 0.05$). #Significant difference from respective T180 ($P < 0.05$). *Significant difference from LETO ($P < 0.05$). † Significant difference from OLETF ($P < 0.05$). ‡ Significant difference from ARB ($P < 0.05$).

ARBM treated rats but increased them 98% at T360 (Fig. 7D).

4.9. Nitrotyrosine increases in diabetic animals but is ameliorated with AT1 antagonism

Total nitrotyrosine and parkin were measured to determine the amount of cellular damage accrued and potential for mitophagy. Total nitrotyrosine levels increase 35% in OLETF rats compared to LETO (Fig. 8A). Total nitrotyrosine levels were 37% lower in ARB treated animals compared to OLETF (Fig. 8A). Total parkin levels increased 34% in OLETF rats compared to LETO (Fig. 8B). ARBM treatment increased parkin levels 27% in OLETF (Fig. 8B). Total nitrotyrosine levels increased 35% in OLETF rats compared to LETO, while ARB treatment lowered Nitrotyrosine levels 37% (Fig. 8B).

5. Discussion

The CDC states that T2DM afflicts over 29 million individuals in the United States. The majority of these people experience cardiovascular-related dysfunctions with as many as 70% of individuals with T2DM dying from cardiovascular related complications [27]. During the development of T2DM, endogenous antioxidant production and activity is impaired likely from impaired Nrf2 signaling along with mitochondrial dysfunction, which is disconcerting due to the heart's highly oxidative nature [28,29]. In the present study Nrf2-related genes were lowered in T2DM hearts and did not increase in response to glucose as the lean control hearts did. Furthermore, ARB treatment lowered ventricular mass, restored some of Nrf2's target genes, and increased several proteins essential to GSH production. Removal of ARB treatment was detrimental in that the ventricular mass returned to T2DM levels in just four weeks and a lack of response was seen in GSH in after the glucose challenge.

During T2DM, the inappropriate activation of AT1 increases in arterial blood pressure and NADPH oxidase activation, which increases oxidant generation [30,31]. Nrf2 is a transcription factor that controls expression of a wide variety of genes some of which are responsible for removal of cellular oxidants [32]. We proposed that Nrf2 would be activated and increase its target genes in response to glucose because hyperglycemia has been implicated in increasing oxidant production [4]. Nrf2 transcripts increased in lean control animals in response to glucose, while diabetic animals had lowered transcript levels and did not respond with glucose. No changes in nuclear Nrf2 protein were observed at any of the measurement periods in the study; however, acetylation of Nrf2 was increased in ARB treated animals, while no changes were observed in response to glucose. Acetylation of Nrf2 has been implicated in initiating gene expression after Nrf2 has been bound to the EpRE [33,34]. Keap1 levels were unchanged in diabetic hearts; however, ARB treatment lowered static Keap1 protein, while ARBM treatment increased it indicating that suppression of Nrf2 in the cytosol may be lower with ARB treatment, but not with the removal of ARB. GSK3β protein was increased statically in diabetic hearts and was unchanged in response to glucose suggesting that nuclear degradation of Nrf2 may be occurring via Beta-Transducin Repeat Containing E3 Ubiquitin Protein Ligase (β-TrCP) [35,36]. Furthermore, Nrf2 nuclear binding is regulated by both Bach1 and c-Myc, which act as repressor proteins inhibiting Nrf2's binding to the EpRE in the nucleus [37–39]. Transcripts were lower for both of these repressors in the diabetic animals despite the lack of nuclear accumulation. Together these data suggest that ARB treatment may confer some benefit to Nrf2 signaling during T2DM due to the increase in Nrf2 acetylation and reduction in some of the genes responsible for its repression.

GSH is the most abundant non-enzymatic antioxidant within the body and its production is primarily controlled by GCLC and GCLM, which are responsible for the formation of GCL. GCL generates γ-glutamyl cysteine from glutamate and cysteine prior to the addition of

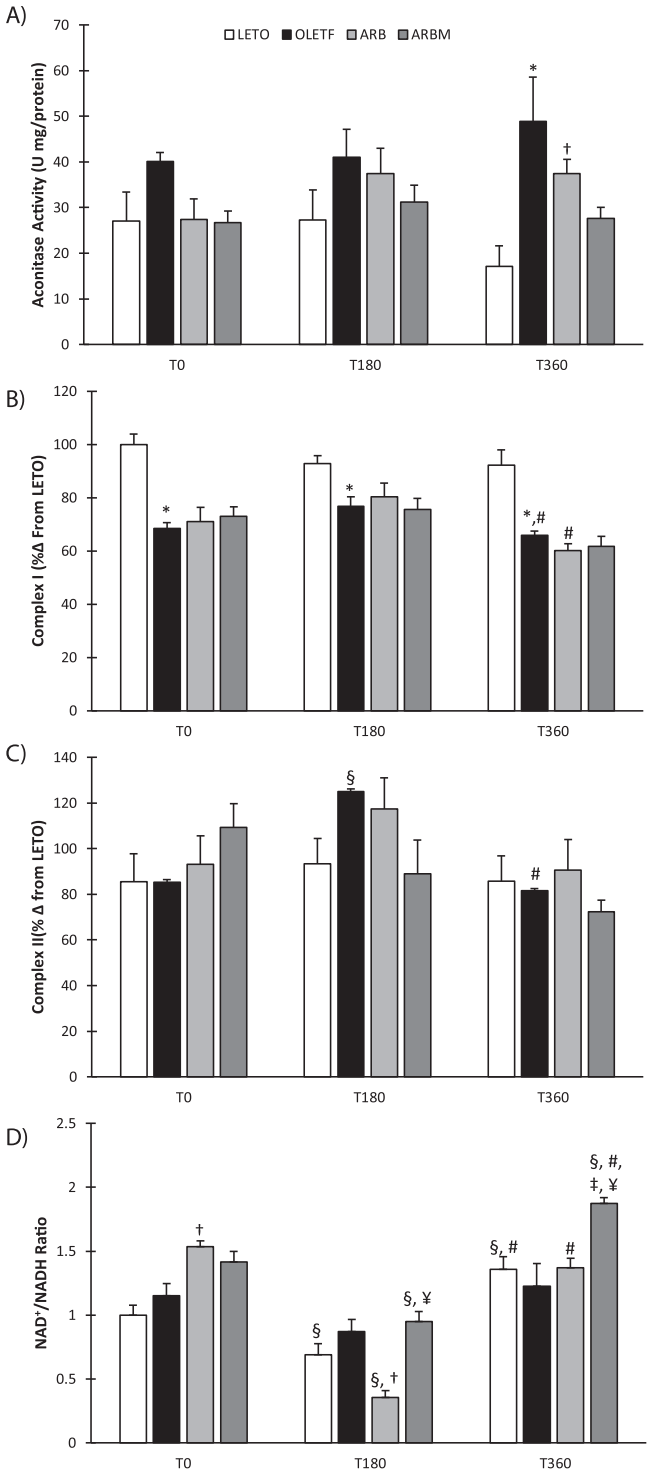

Fig. 7. Mitochondrial function and NADH status. Mean ± SEM values of A) Aconitase activity, B) Complex I activity, C) Complex II activity, and D) NAD^+/NADH ratios values post glucose challenge in Long Evans Tokushima Otsuka (LETO; n = 6), Otsuka Long Evans Tokushima Fatty (OLETF; n = 8), OLETF + angiotensin receptor type 1 blocker 8 weeks (ARB; n = 8) rats, and OLETF + angiotensin receptor type 1 blocker 4 weeks, then removed (ARBM; n = 8) rats. §Significant difference from respective T0 ($P < 0.05$). #Significant difference from respective T180 ($P < 0.05$). *Significant difference from LETO ($P < 0.05$). † Significant difference from OLETF ($P < 0.05$). ¥ Significant difference between OLETF and ARBM ($P < 0.05$).

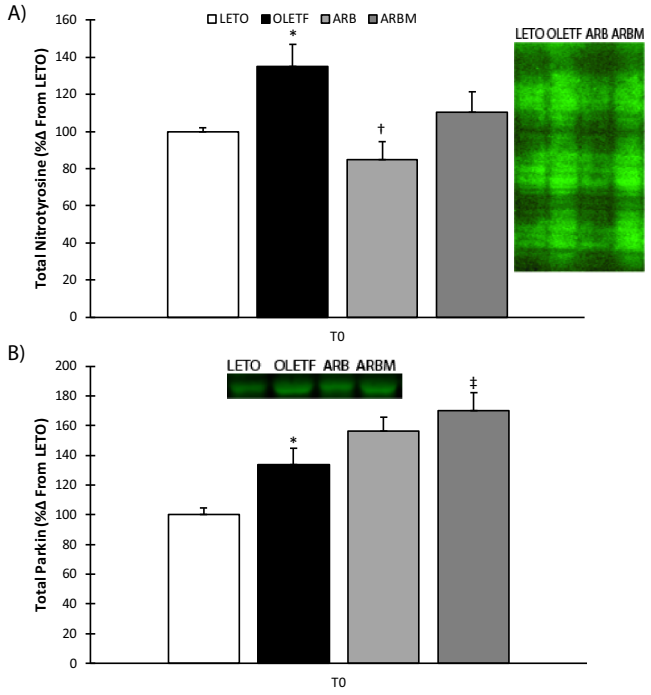

Fig. 8. Total nitrotyrosine and parkin content. Mean ± SEM values of A) total nitrotyrosine, and B) total parkin values post glucose challenge in Long Evans Tokushima Otsuka (LETO; n = 6), Otsuka Long Evans Tokushima Fatty (OLETF; n = 8), OLETF + angiotensin receptor type 1 blocker 8 weeks (ARB; n = 8) rats, and OLETF + angiotensin receptor type 1 blocker 4 weeks, then removed (ARBM; n = 8) rats. *Significant difference from LETO ($P < 0.05$). † Significant difference from OLETF ($P < 0.05$).

glutamate by glutathione synthetase to generate GSH [40]. GCLC transcripts and protein were suppressed statically in diabetic animals. Glucose increased transcripts in both lean stain control animals and diabetic animals to a lesser extent. GCLM is the rate-limiting subunit to GCL formation and subsequent GSH formation [40]. GCLM transcripts and protein levels were also reduced statically in diabetic animals with no change after the glucose challenge indicating that GCLM is less inducible during T2DM. However, ARB treatment increased GCLM transcripts in response to glucose and GCLM protein was elevated statically indicating that AT1 activation may be detrimental to induction of Nrf2-related genes during T2DM. Total GSH content increased in T2DM and ARB animals after the glucose challenge suggesting that blocking the AT1 receptor provides no benefit in GSH's induction; however, the removal of ARB had no appreciable effect on the GSH response to glucose. This suggests that the production of GSH is needed during large influxes of glucose in diabetic animals. Gamma glutamyl transferase is an enzyme responsible for breaking down GSH to allow import of cysteine for intracellular GSH synthesis [41]. Plasma GGT activity increased in all groups post glucose challenge suggesting that import of cysteine is needed for GSH's production.

Several of the antioxidant enzymes involved in the glutathione cycle were also measured in the cytosol and the mitochondria to gain insight about the dynamic responses that occur in each compartment of the cell to a glucose challenge. No changes in cytosolic GPx or GST were observed, but GR levels were reduced in all groups except for control. Glucose increased GR activity in the lean animals suggesting that reduction of GSSG to GSH likely occurs in the cytosol during the glucose challenge and that during T2DM condition the reduction of GSSG is less efficient. In the mitochondria, GR activity increased in T2DM animals in response to glucose, but were even higher in ARB treated animals suggesting that AT1 antagonism aids the mitochondria in reducing GSSG back to GSH. This is important for mitochondrial protection, which houses approximately 10% of the total GSH pool [42]. In animals

where AT1 blockade was removed, GR, GST, and GPx did not change or were suppressed in response to glucose suggesting that removal of AT1 blockade may be detrimental by impairing GSSG reduction. Together, this suite of data illustrates that the GSH cycle is impacted in the heart of T2DM animals and that ARB bestows some benefit. This is further corroborated by the increase in total nitrotyrosine content in T2DM hearts and reduction with AT1 antagonism.

Glucose-6-phosphate dehydrogenase (G6PD) and 6-phosphogluconate dehydrogenase (PGD) are the two enzymes in the oxidative phase of the pentose phosphate pathway responsible for NADPH replenishment. PGD levels rose in control animals in response to glucose further demonstrating that glucose induces Nrf2-related gene expression in normal hearts. G6PD and PGD transcripts were lowered in T2DM animals compared to control with no changes in response to glucose. A corresponding increase in $NADP^+$/NADPH ratio at T360 further support the idea that the pool of NADPH is shifting to a more oxidized state, which may be problematic since enzymes such as GR rely on NADPH to reduce GSSG. These data suggest that during T2DM the induction of Nrf2-related gene expression by glucose is impaired, which can potentially diminish the capacity of the cell to replenish NADPH levels and ultimately impair cellular oxidative balance.

Ratios of NAD^+/NADH were also measured to gain a better understanding of the diabetic heart's redox potentials during a glucose challenge. The NADH pool is larger than that of NADPH and is generally kept in a reduced state; however, when NADPH is low, a shift in favor of oxidation of NADH may occur where electrons from NADH are donated to NADPH through nicotinamide nucleotide transhydrogenase [42,43]. NAD^+/NADH levels shift to a more reduced state at 3 h (T180) in all groups and become more oxidized at 6 h (T360) in all groups except for the T2DM animals suggesting that NADH may be converted to NADPH during a glucose load, which may aid GR's activity.

Mitochondria are susceptible to damage during the transition to T2DM and are known to have impaired function [28]. Previously we demonstrated that in insulin resistant OLETF hearts, mitochondrial function is decreased, while nitrotyrosine and 4-hydroxynonal levels increased [15,16]. While it's still not completely clear, it's believed that changes in mitochondrial oxidant production may generate local damage, lowering mitochondrial enzyme efficiency and increasing mitophagy [43–45]. Aconitase is among the most notably oxidized mitochondrial enzymes because of its high reactivity due to its iron content [5,46]. Aconitase activity increased in response to glucose in the diabetic animals at 6 h (T360) with a reduction in activity in ARB treated animals. This was surprising as we've demonstrated the enzymes reduction in activity in insulin resistant animals [15,16]. Complex I activity was reduced in diabetic animals and in treatment groups while complex II activity did not show any strain effects. It's possible that any changes that occurred in activity occurred prior to the 3-h measurement period. Furthermore, complex I and II have been reported to undergo reverse or partial oxidation of oxygen resulting in increased oxidant production [6,47,48]. Pink1 and parkin have been reported to initiate mitophagy in the neural tissue [48,49]. Pink1 accumulates upon the surface of the mitochondria allowing for parkin to translocate into mitochondria to initiate mitophagy of damaged mitochondria [43]. Total parkin levels increased in diabetic animals, while AT1 antagonism provided no discernable benefit. Removal of ARB, however, increased parkin levels beyond those in diabetic animals suggesting that the reactivation of AT1 contributes to mitochondrial damage and/or mitophagy, and more importantly, exacerbates the condition. Hypertension has been thought to contribute to mitochondrial damage through a loss in cardiolipin for electron transport chain complex assembly [50]. These data suggest that in the early stages of T2DM damage to the mitochondria impairs complex I function, increasing damage and potentially mitophagy.

Here we've demonstrated that during the early stages of T2DM, the induction of Nrf2-related genes is impaired in diabetic animals in response to glucose, while AT1 antagonism confers some benefit to restoring and/or maintaining Nrf2-related gene transcription. GSH levels increased in both T2DM and ARB treated animals during the glucose challenge, but GR activity is heightened in ARB treated animals suggesting that sustained activation of AT1 in the diabetic heart impairs the cellular response to a glucose load. The implications here are that frequent post-prandial bouts of hyperglycemia in diabetics may incrementally lead to irreversible damage of mitochondrial function in the heart and ultimately more severe cardiovascular complications. Furthermore, removal of AT1 antagonism impairs the dynamic responses of many key proteins within these detoxification systems, rendering the cellular response to glucose less efficient/effective and potentially inactive. These data would substantiate previous findings that "cellular memory" associated with AT1 antagonism results in detrimental effects on the diabetic heart as ventricular hypertrophy and hypertension returned to diabetic levels within only four weeks off of treatment. While over-activation of AT1 contributes to the hypertension associated with the T2DM condition, these data demonstrate that the consequences of AT1 activation during T2DM go well beyond sustaining elevated arterial pressure, but also include impaired mitochondrial function, Nrf2-mediated events, and cellular homeostasis in the diabetic heart.

Acknowledgements

M. Thorwald, J. Godoy-Lugo, G. Rodriguez, and M. Rodriguez were supported by NIH NCMHD9T37MD001480.

Appendix A. Supplementary material

Supplementary data associated with this article can be found in the online version at doi:10.1016/j.freeradbiomed.2018.10.405.

References

[1] Diabetes Mellitus: A major risk factor for cardiovascular disease: a joint editorial statement by the American Diabetes Association; the National Heart, Lung, and Blood Institute; the Juvenile Diabetes Foundation International; the National Institute of Diabetes and Digestive and Kidney Diseases; and the American Heart Association, Circulation, 100, 1999, pp. 1132–1133. ⟨https://dx.doi.org/10.1161/01.CIR.100.10.1132⟩.

[2] K. Kawano, T. Hirashima, S. Mori, Y. Saitoh, M. Kurosumi, T. Natori, Spontaneous long-term hyperglycemic rat with diabetic complications. Otsuka Long-Evans Tokushima Fatty (OLETF) strain, Diabetes 41 (1992) 1422–1428.

[3] M. Dunlop, Aldose reductase and the role of the polyol pathway in diabetic nephropathy, Kidney Int. Suppl. 77 (2000) S3–S12.

[4] G. Giacchetti, L.A. Sechi, S. Rilli, R.M. Carey, The renin-angiotensin-aldosterone system, glucose metabolism and diabetes, Trends Endocrinol. Metab. Tem. 16 (2005) 120–126, https://doi.org/10.1016/j.tem.2005.02.003.

[5] P.R. Gardner, I. Fridovich, Superoxide sensitivity of the Escherichia coli aconitase, J. Biol. Chem. 266 (1991) 19328–19333.

[6] K.R. Pryde, J. Hirst, Superoxide is produced by the reduced flavin in mitochondrial complex I a single, unified mechanism that applies during both forward and reverse electron transfer, J. Biol. Chem. 286 (2011) 18056–18065, https://doi.org/10.1074/jbc.M110.186841.

[7] J. Vásquez-Vivar, B. Kalyanaraman, M.C. Kennedy, Mitochondrial aconitase is a source of hydroxyl radical an electron spin resonance investigation, J. Biol. Chem. 275 (2000) 14064–14069, https://doi.org/10.1074/jbc.275.19.14064.

[8] W. Li, S. Yu, T. Liu, J.-H. Kim, V. Blank, H. Li, A.-N.T. Kong, Heterodimerization with small maf proteins enhances nuclear retention of Nrf2 via masking the NESzip motif, Biochim. Biophys. Acta 2008 (1783) 1847–1856, https://doi.org/10.1016/j.bbamcr.2008.05.024.

[9] M.B. Kannan, V. Solovieva, V. Blank, The small MAF transcription factors MAFF, MAFG and MAFK: current knowledge and perspectives, Biochim. Biophys. Acta 2012 (1823) 1841–1846, https://doi.org/10.1016/j.bbamcr.2012.06.012.

[10] M.C. Jaramillo, D.D. Zhang, The emerging role of the Nrf2-Keap1 signaling pathway in cancer, Genes Dev. 27 (2013) 2179–2191, https://doi.org/10.1101/gad.225680.113.

[11] G.V. Velmurugan, N.R. Sundaresan, M.P. Gupta, C. White, Defective Nrf2-dependent redox signalling contributes to microvascular dysfunction in type 2 diabetes, Cardiovasc. Res. 100 (2013) 143–150, https://doi.org/10.1093/cvr/cvt125.

[12] A.S. Jiménez-Osorio, A. Picazo, S. González-Reyes, D. Barrera-Oviedo, M.E. Rodríguez-Arellano, J. Pedraza-Chaverri, Nrf2 and redox status in prediabetic and diabetic patients, Int. J. Mol. Sci. 15 (2014) 20290–20305, https://doi.org/10.3390/ijms151120290.

[13] J.M. Luther, N.J. Brown, Renin-angiotensin-aldosterone system and glucose

homeostasis, Trends Pharmacol. Sci. 32 (2011) 734–739, https://doi.org/10.1016/j.tips.2011.07.006.
[14] M.L. Onozato, A. Tojo, A. Goto, T. Fujita, C.S. Wilcox, Oxidative stress and nitric oxide synthase in rat diabetic nephropathy: effects of ACEI and ARB, Kidney Int. 61 (2002) 186–194, https://doi.org/10.1046/j.1523-1755.2002.00123.x.
[15] M. Thorwald, R. Rodriguez, A. Lee, B. Martinez, J. Peti-Peterdi, D. Nakano, A. Nishiyama, R.M. Ortiz, Angiotensin receptor blockade improves cardiac mitochondrial activity in response to an acute glucose load in obese insulin resistant rats, Redox Biol. 14 (2018) 371–378, https://doi.org/10.1016/j.redox.2017.10.005.
[16] J.P. Vázquez-Medina, I. Popovich, M.A. Thorwald, J.A. Viscarra, R. Rodriguez, J.G. Sonanez-Organis, L. Lam, J. Peti-Peterdi, D. Nakano, A. Nishiyama, R.M. Ortiz, Angiotensin receptor-mediated oxidative stress is associated with impaired cardiac redox signaling and mitochondrial function in insulin-resistant rats, Am. J. Physiol. Heart Circ. Physiol. 305 (2013) H599–H607, https://doi.org/10.1152/ajpheart.00101.2013.
[17] H. Sasamura, H. Itoh, 'Memory' and 'legacy' in hypertension and lifestyle-related diseases, Hypertens. Res. (2012), https://doi.org/10.1038/h.2011.222.
[18] H. Sasamura, K. Hayashi, K. Ishiguro, H. Nakaya, T. Saruta, H. Itoh, Prevention and regression of hypertension: role of renal microvascular protection, Hypertens. Res. 32 (2009) 658–664, https://doi.org/10.1038/h.2009.85.
[19] R. Rodriguez, J.N. Minas, J.P. Vazquez-Medina, D. Nakano, D.G. Parkes, A. Nishiyama, R.M. Ortiz, Chronic AT1 blockade improves glucose homeostasis in obese OLETF rats, J. Endocrinol. 237 (2018) 271–284, https://doi.org/10.1530/JOE-17-0678.
[20] R. Rodriguez, J.A. Viscarra, J.N. Minas, D. Nakano, A. Nishiyama, R.M. Ortiz, Angiotensin receptor blockade increases pancreatic insulin secretion and decreases glucose intolerance during glucose supplementation in a model of metabolic syndrome, Endocrinology 153 (2012) 1684–1695, https://doi.org/10.1210/en.2011-1885.
[21] P. Montez, J.P. Vázquez-Medina, R. Rodríguez, M.A. Thorwald, J.A. Viscarra, L. Lam, J. Peti-Peterdi, D. Nakano, A. Nishiyama, R.M. Ortiz, Angiotensin receptor blockade recovers hepatic ucp2 expression and aconitase and SDH activities and ameliorates hepatic oxidative damage in insulin resistant rats, Endocrinology 153 (2012) 5746–5759, https://doi.org/10.1210/en.2012-1390.
[22] Y.K. Oh, K.W. Joo, J.W. Lee, U.S. Jeon, C.S. Lim, J.S. Han, M.A. Knepper, K.Y. Na, Altered renal sodium transporter expression in an animal model of type 2 diabetes mellitus, J. Korean Med. Sci. 22 (2007) 1034–1041, https://doi.org/10.3346/jkms.2007.22.6.1034.
[23] I. Rahman, A. Kode, S.K. Biswas, Assay for quantitative determination of glutathione and glutathione disulfide levels using enzymatic recycling method, Nat. Protoc. 1 (2007) 3159–3165, https://doi.org/10.1038/nprot.2006.378.
[24] Y. Hiraku, M. Murata, S. Kawanishi, Determination of intracellular glutathione and thiols by high performance liquid chromatography with a gold electrode at the femtomole level: comparison with a spectroscopic assay, Biochim. Biophys. Acta BBA – Gen. Subj. 1570 (2002) 47–52, https://doi.org/10.1016/S0304-4165(02)00152-6.
[25] I. Dimauro, T. Pearson, D. Caporossi, M.J. Jackson, A simple protocol for the subcellular fractionation of skeletal muscle cells and tissue, BMC Res. Notes 5 (2012) 513, https://doi.org/10.1186/1756-0500-5-513.
[26] J.S. Thacker, D.H. Yeung, W.R. Staines, J.G. Mielke, Total protein or high-abundance protein: which offers the best loading control for Western blotting? Anal. Biochem. 496 (2016) 76–78, https://doi.org/10.1016/j.ab.2015.11.022.
[27] M. Laakso, Cardiovascular disease in Type 2 diabetes from population to man to mechanisms, Diabetes Care 33 (2010) 442–449, https://doi.org/10.2337/dc09-0749.
[28] B.B. Lowell, G.I. Shulman, Mitochondrial dysfunction and type 2 diabetes, Science 307 (2005) 384–387, https://doi.org/10.1126/science.1104343.
[29] M.K. Montgomery, N. Turner, Mitochondrial dysfunction and insulin resistance: an update, Endocr. Connect. 4 (2014) R1–R15, https://doi.org/10.1530/EC-14-0092.
[30] K.K. Griendling, C.A. Minieri, J.D. Ollerenshaw, R.W. Alexander, Angiotensin II stimulates NADH and NADPH oxidase activity in cultured vascular smooth muscle cells, Circ. Res. 74 (1994) 1141–1148, https://doi.org/10.1161/01.RES.74.6.1141.
[31] J.R. Sowers, Diabetes mellitus and vascular disease, Hypertens. (Dallas Tex. 1979) 61 (2013) 943–947, https://doi.org/10.1161/HYPERTENSIONAHA.111.00612.
[32] X.-L. Chen, C. Kunsch, Induction of cytoprotective genes through Nrf2/antioxidant response element pathway: a new therapeutic approach for the treatment of inflammatory diseases, Curr. Pharm. Des. 10 (2004) 879–891.
[33] Y. Kawai, L. Garduño, M. Theodore, J. Yang, I.J. Arinze, Acetylation-deacetylation of the transcription factor Nrf2 (Nuclear factor erythroid 2-related factor 2) regulates its transcriptional activity and nucleocytoplasmic localization, J. Biol. Chem. 286 (2011) 7629–7640, https://doi.org/10.1074/jbc.M110.208173.
[34] Z. Sun, Y.E. Chin, D.D. Zhang, Acetylation of Nrf2 by p300/CBP augments promoter-specific dna binding of Nrf2 during the antioxidant response, Mol. Cell. Biol. 29 (2009) 2658–2672, https://doi.org/10.1128/MCB.01639-08.
[35] P. Rada, A.I. Rojo, S. Chowdhry, M. McMahon, J.D. Hayes, A. Cuadrado, SCF/β-TrCP promotes glycogen synthase kinase 3-dependent degradation of the Nrf2 transcription factor in a Keap1-independent manner, Mol. Cell. Biol. 31 (2011) 1121–1133, https://doi.org/10.1128/MCB.01204-10.
[36] S. Chowdhry, Y. Zhang, M. McMahon, C. Sutherland, A. Cuadrado, J.D. Hayes, Nrf2 is controlled by two distinct β-TrCP recognition motifs in its Neh6 domain, one of which can be modulated by GSK-3 activity, Oncogene 32 (2013) 3765–3781, https://doi.org/10.1038/onc.2012.388.
[37] S. Levy, H.J. Forman, C-Myc is a Nrf2-interacting protein that negatively regulates phase II genes through their electrophile responsive elements, IUBMB Life 62 (2010) 237–246, https://doi.org/10.1002/iub.314.
[38] S. Dhakshinamoorthy, A.K. Jain, D.A. Bloom, A.K. Jaiswal, Bach1 competes with Nrf2 leading to negative regulation of the antioxidant response element (ARE)-mediated NAD(P)H: quinone oxidoreductase 1 gene expression and induction in response to antioxidants, J. Biol. Chem. 280 (2005) 16891–16900, https://doi.org/10.1074/jbc.M500166200.
[39] L. Zhou, H. Zhang, K.J.A. Davies, H.J. Forman, Aging-related decline in the induction of Nrf2-regulated antioxidant genes in human bronchial epithelial cells, Redox Biol. 14 (2018) 35–40, https://doi.org/10.1016/j.redox.2017.08.014.
[40] C.C. Franklin, D.S. Backos, I. Mohar, C.C. White, H.J. Forman, T.J. Kavanagh, Structure, function, and post-translational regulation of the catalytic and modifier subunits of glutamate cysteine ligase, Mol. Asp. Med. 30 (2009) 86–98, https://doi.org/10.1016/j.mam.2008.08.009.
[41] H. Zhang, H.J. Forman, J. Choi, Gamma-glutamyl transpeptidase in glutathione biosynthesis, Methods Enzymol. 401 (2005) 468–483, https://doi.org/10.1016/S0076-6879(05)01028-1.
[42] M.J. Meredith, D.J. Reed, Status of the mitochondrial pool of glutathione in the isolated hepatocyte, J. Biol. Chem. 257 (1982) 3747–3753.
[43] X. Zheng, T. Hunter, Parkin mitochondrial translocation is achieved through a novel catalytic activity coupled mechanism, Cell Res. 23 (2013) 886–897, https://doi.org/10.1038/cr.2013.66.
[44] T. Finkel, Signal transduction by mitochondrial oxidants, J. Biol. Chem. 287 (2012) 4434–4440, https://doi.org/10.1074/jbc.R111.271999.
[45] R.S. Balaban, S. Nemoto, T. Finkel, Mitochondria, oxidants, and aging, Cell 120 (2005) 483–495, https://doi.org/10.1016/j.cell.2005.02.001.
[46] M.C. Kennedy, M.H. Emptage, J.L. Dreyer, H. Beinert, The role of iron in the activation-inactivation of aconitase, J. Biol. Chem. 258 (1983) 11098–11105.
[47] C.L. Quinlan, A.L. Orr, I.V. Perevoshchikova, J.R. Treberg, B.A. Ackrell, M.D. Brand, Mitochondrial complex II can generate reactive oxygen species at high rates in both the forward and reverse reactions, J. Biol. Chem. 287 (2012) 27255–27264, https://doi.org/10.1074/jbc.M112.374629.
[48] E. Murphy, H. Ardehali, R.S. Balaban, F. DiLisa, G.W. Dorn, R.N. Kitsis, K. Otsu, P. Ping, R. Rizzuto, M.N. Sack, D. Wallace, R.J. Youle, American Heart Association council on basic cardiovascular sciences, council on clinical cardiology, and council on functional genomics and translational biology, mitochondrial function, biology, and role in disease: a scientific statement from the American Heart Association, Circ. Res. 118 (2016) 1960–1991, https://doi.org/10.1161/RES.0000000000000104.
[49] A.M. Pickrell, R.J. Youle, The roles of PINK1, parkin, and mitochondrial fidelity in Parkinson's disease, Neuron 85 (2015) 257–273, https://doi.org/10.1016/j.neuron.2014.12.007.
[50] A. Eirin, A. Lerman, L.O. Lerman, Mitochondrial injury and dysfunction in hypertension-induced cardiac damage, Eur. Heart J. 35 (2014) 3258–3266, https://doi.org/10.1093/eurheartj/ehu436.